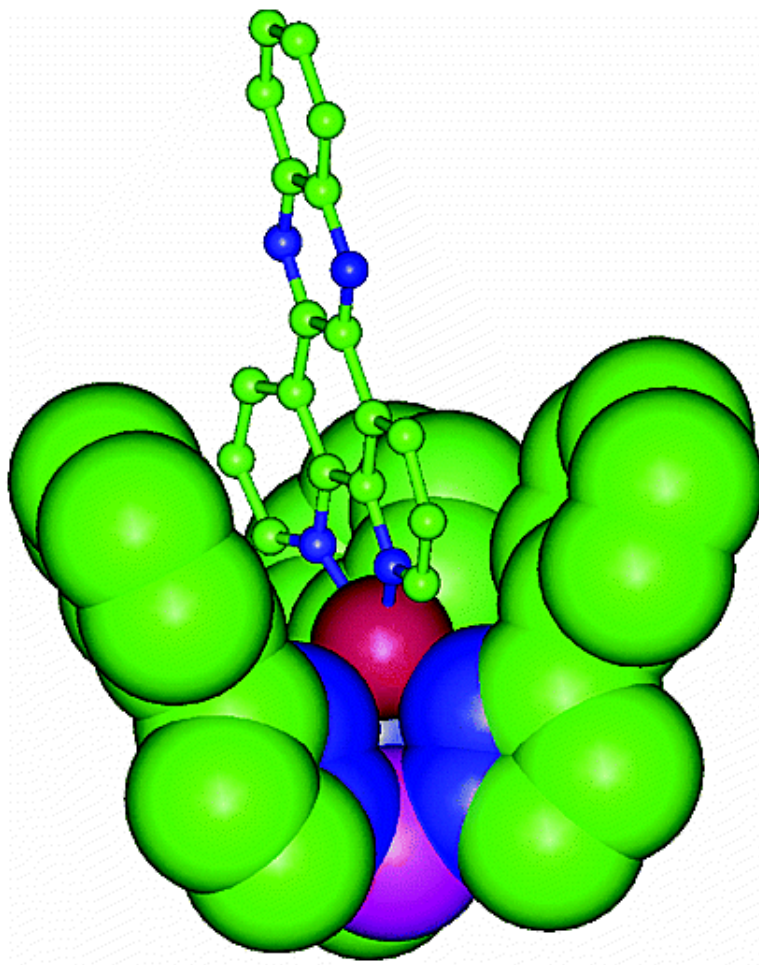


## Effect of Steric Encumbrance of Tris(3-phenylpyrazolyl)borate on the Structure and Properties of Ternary Copper(II) Complexes Having N,N-Donor Heterocyclic Bases

Shanta Dhar, Pattubala A. N. Reddy, Munirathinam Nethaji,  
Subramony Mahadevan, Manas K. Saha, and Akhil R. Chakravarty

*Inorg. Chem.*, **2002**, 41 (13), 3469-3476 • DOI: 10.1021/ic0201396

Downloaded from <http://pubs.acs.org> on January 26, 2009



More About This Article



**ACS Publications**  
High quality. High impact.

Additional resources and features associated with this article are available within the HTML version:

- Supporting Information
- Links to the 3 articles that cite this article, as of the time of this article download
- Access to high resolution figures
- Links to articles and content related to this article
- Copyright permission to reproduce figures and/or text from this article

[View the Full Text HTML](#)



# Effect of Steric Encumbrance of Tris(3-phenylpyrazolyl)borate on the Structure and Properties of Ternary Copper(II) Complexes Having N,N-Donor Heterocyclic Bases

Shanta Dhar,<sup>†</sup> Pattubala A. N. Reddy,<sup>†</sup> Munirathinam Nethaji,<sup>†</sup> Subramony Mahadevan,<sup>‡</sup> Manas K. Saha,<sup>†</sup> and Akhil R. Chakravarty<sup>\*†</sup>

Department of Inorganic & Physical Chemistry and Department of Molecular Reproduction, Development & Genetics, Indian Institute of Science, Bangalore 560012, India

Received February 18, 2002

Complexes of formulation  $[\text{Cu}(\text{Tp}^{\text{Ph}})(\text{L})](\text{ClO}_4)$  (**1–4**), where  $\text{Tp}^{\text{Ph}}$  is anionic tris(3-phenylpyrazolyl)borate and L is N,N-donor heterocyclic base, viz. 2,2'-bipyridine (bpy, **1**), 1,10-phenanthroline (phen, **2**), dipyrrodoquinoxaline (dpq, **3**), and dipyrrodoquinazoline (dppz, **4**), are prepared from a reaction of copper(II) acetate-hydrate with  $\text{KTp}^{\text{Ph}}$  and L in  $\text{CH}_2\text{Cl}_2$  and isolated as perchlorate salts. The complexes are characterized by analytical, structural, and spectral methods. The crystal structures of complexes **1–4** show the presence of discrete cationic complexes having the metal,  $\text{Tp}^{\text{Ph}}$ , and L in a 1:1:1 ratio and a noncoordinating perchlorate anion. The complexes have a square-pyramidal 4 + 1 coordination geometry in which two nitrogens of L and two nitrogens of the  $\text{Tp}^{\text{Ph}}$  ligand occupy the basal plane and one nitrogen of  $\text{Tp}^{\text{Ph}}$  binds at the axial site. Complexes **3** and **4** display distortion from the square-pyramidal geometry. The Cu–N distances for the equatorial and axial positions are  $\sim 2.0$  and  $2.2$  Å, respectively. The phenyl groups of  $\text{Tp}^{\text{Ph}}$  form a bowl-shaped structure that encloses the  $\{\text{CuL}\}$  moiety. The steric encumbrance is greater for the bpy and phen ligands compared to that for dpq and dppz. The one-electron paramagnetic complexes ( $\mu \approx 1.8 \mu_{\text{B}}$ ) exhibit axial EPR spectra in  $\text{CH}_2\text{Cl}_2$  glass at 77 K giving  $g_{\parallel}$  and  $g_{\perp}$  values of  $\sim 2.18$  ( $A_{\parallel} = 128$  G) and  $\sim 2.07$ . The data suggest a  $\{d_{x^2-y^2}\}^1$  ground state. The complexes are redox-active and display a quasireversible cyclic voltammetric response for the Cu(II)/Cu(I) couple near 0.0 V versus SCE with an  $i_{\text{pc}}/i_{\text{pa}}$  ratio of unity in  $\text{CH}_2\text{Cl}_2$  or DMF–0.1 M TBAP. The  $E_{1/2}$  values of the couple vary in the order **4** > **3** > **2** > **1**. A profound effect of steric encumbrance caused by the  $\text{Tp}^{\text{Ph}}$  ligand is observed in the reactivity of **1–4** with the calf thymus (CT) and supercoiled (SC) DNA. Complexes **2–4** show similar binding to CT DNA. The propensity for the SC DNA cleavage varies as **4** > **3** > **2**. The bpy complex does not show any significant binding or cleavage of DNA. Mechanistic investigations using distamycin reveal minor groove binding for **2** and **3** and a major groove binding for **4**. The scission reactions that are found to be inhibited by hydroxyl radical scavenger DMSO are likely to proceed through sugar hydrogen abstraction pathways.

## Introduction

Coordination chemistry of tris(pyrazolyl)borate (Tp) ligand spans major areas of inorganic chemistry.<sup>1–7</sup> The capping

tridentate ligand has been used as a substitute for the six-electron donor  $\eta^5$ -cyclopentadienyl anion or  $\eta^6$ -arenes in organometallic chemistry.<sup>1b,3,5</sup> The advantage of having

\* To whom correspondence should be addressed. E-mail: arc@ipc.iisc.ernet.in.

<sup>†</sup> Department of Inorganic & Physical Chemistry.

<sup>‡</sup> Department of Molecular Reproduction, Development & Genetics.

- (1) Trofimenko, S. *Prog. Inorg. Chem.* **1986**, *34*, 115. (b) Trofimenko, S. *Inorg. Chem.* **1969**, *8*, 2675. (c) Trofimenko, S. *J. Am. Chem. Soc.* **1966**, *88*, 1842; **1967**, *89*, 3170. (d) Trofimenko, S. *Chem. Rev.* **1972**, *72*, 497. (e) Trofimenko, S. *Acc. Chem. Res.* **1971**, *4*, 17. (f) Trofimenko, S. *Chem. Rev.* **1993**, *93*, 943.  
(2) Niedenzu, K.; Trofimenko, S. *Top. Curr. Chem.* **1986**, *131*, 1.

- (3) (a) Byers, P. K.; Cauty, A. J.; Honeyman, R. T. *Adv. Organomet. Chem.* **1992**, *34*, 1. (b) Guo, S.; Peters, F.; De Biani, F. F.; Bats, J. W.; Herdtweck, E.; Zanello, P.; Wagner, M. *Inorg. Chem.* **2001**, *40*, 4928.  
(4) Kitajima, N.; Tolman, W. B. *Prog. Inorg. Chem.* **1995**, *43*, 419.  
(5) Shaver, A. In *Comprehensive Coordination Chemistry*; Wilkinson, G., Gilliard, R. D., McCleverty, J. A., Eds.; Pergamon Press: Oxford, 1987; Vol. 2; pp 245–259.  
(6) Parkin, G. *Adv. Inorg. Chem.* **1996**, *42*, 291.  
(7) Hikichi, S.; Akita, M.; Moro-oka, Y. *Coord. Chem. Rev.* **2000**, *198*, 61.

various degrees of steric constraints generated by the substituents at the 3 and 5 positions of the pyrazolyl ring of Tp has made this ligand system very effective in the synthesis of model complexes for the active sites of several non-heme metalloproteins.<sup>4,8–10</sup> The ( $\mu$ -oxo/hydroxo)bis( $\mu$ -carboxylato)-diiron(III) complexes having two facial Tp ligands mimic the structural features of the diiron core in the invertebrate respiratory protein hemerythrin.<sup>10c–e</sup> Again, the synthesis of structural and functional mimics of the dioxygen binding protein hemocyanin is achieved using disubstituted Tp ligands in crystallizing a complex having a  $[\text{Cu}_2(\mu\text{-}\eta^2\text{-}\eta^2\text{-O}_2)]^{2+}$  core.<sup>11</sup> The anionic ligand HB(3-*t*-Bu-5-*i*-Prpz)<sub>3</sub> has been successfully used in stabilizing a superoxide moiety showing  $\eta^2$ -mode of bonding to copper.<sup>12</sup> The ligand system has also been used in the preparation of an alkylperoxide-bound copper complex.<sup>13</sup> The present work stems from our interest in preparing copper(II) complexes having phenyl substituted tris(pyrazolyl)borate anion and chelating N-donor heterocyclic bases to study the steric effect of the Tp<sup>Ph</sup> ligand on the coordination geometry and nuclease activity of the ternary complexes.

Metallointercalators having planar N-donor heterocyclic bases are used as photochemical and chemical reagents in nucleic acids chemistry.<sup>14–18</sup> The redox-active bis-phen copper complex has found wide application as a chemical nuclease for its ability to nick DNA.<sup>14</sup> Although the true binding of this complex to DNA is presently unknown, it has been suggested that the nuclease activity is related to the partial intercalation or binding of one phen ligand to the minor groove of DNA while the other phen ligand makes favorable contact within the groove.<sup>19</sup> Nuclease activity of the copper complexes primarily depends on two factors, viz.

(i) the redox potential and the reversibility of the Cu(II)/Cu(I) couple, and (ii) the intercalative nature of the complex. Design of redox-active copper complexes as new chemical nucleases is an area of current research interest.<sup>20,21</sup> The ancillary ligand (L) in  $[\text{CuL}(\text{phen})]^{n+}$  can exert profound electronic and steric influence to alter the propensity of the DNA-binding and cleavage in a significant manner compared to its bis(phen) analogue. We have observed a significant variation in the groove selectivity and nuclease activity of  $[\text{Cu}(\text{Tp}^{\text{Ph}})(\text{L})](\text{ClO}_4)$  because of the steric encumbrance caused by tris(3-phenylpyrazolyl)borate anion on the intercalative ability of L [L, 2,2'-bipyridine (bpy), **1**; 1,10-phenanthroline (phen), **2**; dipyrrodoquinoxaline (dpq), **3**; dipyrrodoquinazoline (dppz), **4**]. Herein, we present the synthesis, crystal structures, DNA binding, and cleavage properties of **1–4**.

## Experimental Section

**Materials and Methods.** All reagents and chemicals were purchased from commercial sources. Solvents used for electrochemical and spectroscopic measurements were purified by standard procedures. Potassium salt of tris(3-phenylpyrazolyl)borate (KTP<sup>Ph</sup>) was prepared by a literature method.<sup>22</sup> Dipyrrodo[3,2-d:2',3'-f]-quinoxaline (dpq) and dipyrrodo[3,2-a:2',3'-c]phenazine (dppz) were prepared by reported procedures.<sup>23–25</sup> The calf thymus DNA and supercoiled pUC19 (cesium chloride purified) DNA were purchased from Bangalore Genei (India). Agarose (molecular biology grade), distamycin, and ethidium bromide were from Sigma (USA). Tris-HCl buffer solution was prepared by using deionized, sonicated triple distilled water. Complexes  $[\text{Cu}(\text{phen})_2(\text{H}_2\text{O})](\text{ClO}_4)_2$  and  $[\text{Cu}(\text{Tp}^{\text{Ph}})(\text{O}_2\text{CMe})]$ , used as reference for comparative studies, were prepared by literature methods.<sup>26–28</sup> The elemental analyses were done using a Heraeus CHN-O Rapid instrument. The infrared, electronic, EPR, and fluorescence spectra were recorded on Bruker Equinox 55, Hitachi U-3400, Varian E-109 X-band, and Perkin-Elmer LS-50B spectrophotometers, respectively. Room-temperature magnetic susceptibility data were obtained from a George Associ-

- (8) Blackman, A. G.; Tolman, W. B. In *Structure and Bonding*; Springer-Verlag: Heidelberg, Germany, 2000; Vol. 97, p 173.
- (9) (a) Houser, R. P.; Tolman, W. B. *Inorg. Chem.* **1995**, *34*, 1632. (b) Kimblin, C.; Parkin, G. *Inorg. Chem.* **1996**, *35*, 6912. (c) Xiao, Z.; Young, C. G.; Enemark, J. H.; Wedd, A. G. *J. Am. Chem. Soc.* **1992**, *114*, 9194.
- (10) (a) Lippard, S. J. *Angew. Chem., Int. Ed. Engl.* **1988**, *27*, 344. (b) Kim, K.; Lippard, S. J. *J. Am. Chem. Soc.* **1996**, *118*, 4914. (c) Armstrong, W. H.; Lippard, S. J. *J. Am. Chem. Soc.* **1983**, *105*, 4837. (d) Armstrong, W. H.; Spool, A.; Papaefthymiou, G. C.; Frankel, R. B.; Lippard, S. J. *J. Am. Chem. Soc.* **1984**, *106*, 3653. (e) Armstrong, W. H.; Lippard, S. J. *J. Am. Chem. Soc.* **1984**, *106*, 4632.
- (11) Kitajima, N.; Fujisawa, K.; Moro-oka, Y. *J. Am. Chem. Soc.* **1989**, *111*, 8975. (b) Kitajima, N.; Koda, T.; Hashimoto, S.; Kitagawa, T.; Moro-oka, Y. *J. Chem. Soc., Chem. Commun.* **1988**, 151. (c) Kitajima, N.; Fujisawa, K.; Fujimoto, C.; Moro-oka, Y.; Hashimoto, S.; Kitagawa, T.; Toriumi, K.; Tatsumi, K.; Nakamura, A. *J. Am. Chem. Soc.* **1992**, *114*, 1277. (d) Hikichi, S.; Komatosuzaki, H.; Kitajima, N.; Akita, M.; Mukai, M.; Kitagawa, T.; Moro-oka, Y. *Inorg. Chem.* **1997**, *36*, 266.
- (12) Fujisawa, K.; Tanaka, M.; Moro-oka, Y.; Kitajima, N. *J. Am. Chem. Soc.* **1994**, *116*, 12079.
- (13) Kitajima, N.; Katayama, T.; Fujisawa, K.; Iwata, Y.; Moro-oka, Y. *J. Am. Chem. Soc.* **1993**, *115*, 7872.
- (14) (a) Sigman, D. S.; Bruce, T. W.; Majumder, A.; Sutton, C. L. *Acc. Chem. Res.* **1993**, *26*, 98. (b) Sigman, D. S.; Majumder, A.; Perrin, D. M. *Chem. Rev.* **1993**, *93*, 2295.
- (15) (a) Barton, J. K. *Science* **1986**, *233*, 727. (b) Pyle, A. M.; Barton, J. K. *Prog. Inorg. Chem.* **1990**, *38*, 413.
- (16) Pogogelski, W. K.; Tullius, T. D. *Chem. Rev.* **1998**, *98*, 1089.
- (17) Burrows, C. J.; Muller, J. G. *Chem. Rev.* **1998**, *98*, 1109.
- (18) (a) Meunier, B. *Chem. Rev.* **1992**, *92*, 1411. (b) Pratiel, G.; Bernadou, J.; Meunier, B. *Angew. Chem., Int. Ed. Engl.* **1995**, *34*, 746. (c) Pratiel, G.; Bernadou, J.; Meunier, B. *Adv. Inorg. Chem.* **1998**, *45*, 251.
- (19) (a) Veal, J. M.; Merchant, K.; Rill, R. L. *Nucleic Acids Res.* **1991**, *19*, 3383. (b) Veal, J. M.; Rill, R. L. *Biochemistry* **1991**, *30*, 1132. (c) Veal, J. M.; Rill, R. L. *Biochemistry* **1988**, *27*, 1822. (d) Williams, L. D.; Thivierge, J.; Goldberg, I. H. *Nucleic Acids Res.* **1988**, *16*, 11607. (e) Stockert, J. C. *J. Theor. Biol.* **1989**, *137*, 107.
- (20) (a) Pitie, M.; Horn, J. D. V.; Brion, D.; Burrows, C. J.; Meunier, B. *Bioconjugate Chem.* **2000**, *11*, 892. (b) Chand, D. K.; Schneider, H.-J.; Bencini, A.; Bianchi, A.; Giorgi, C.; Ciattini, S.; Valtancoli, B. *Chem.—Eur. J.* **2000**, *6*, 4001. (c) Lamour, E.; Routier, S.; Bernier, J.-L.; Cateau, J. P.; Bailly, C.; Vezin, H. *J. Am. Chem. Soc.* **1999**, *121*, 1862. (d) Gilbert, B. C.; Silvester, S.; Walton, P. H.; Whitwood, A. C. *J. Chem. Soc., Perkin Trans.* **1999**, 1891. (e) Bando, O.; Teulade-Fichou, M.-P.; Vigneron, J.-P.; Lehn, J.-M. *Chem. Commun.* **1998**, 2349. (f) Nagane, R.; Chilcira, M.; Shindo, H.; Antholine, W. E. *J. Inorg. Biochem.* **2000**, *78*, 243. (g) Chand, D.-K.; Schneider, H.-J.; Agnilar, J.-A.; Escarti, F.; Espana, E.-G.; Luis, S.-V. *Inorg. Chim. Acta* **2001**, *316*, 71.
- (21) Bush, P. M.; Whitehead, J. P.; Pink, C. C.; Gramm, E. C.; Eglin, J. L.; Watton, S. P.; Pence, L. E. *Inorg. Chem.* **2001**, *40*, 1871.
- (22) Eichhorn, D. M.; Armstrong, W. H. *Inorg. Chem.* **1990**, *29*, 3607.
- (23) Bernadou, J.; Pratiel, G.; Bennis, F.; Girardet, M.; Meunier, B. *Biochemistry* **1989**, *28*, 7268.
- (24) Dickeson, J. E.; Summers, L. A. *Aust. J. Chem.* **1970**, *23*, 1023.
- (25) Amouyal, E.; Homs, A.; Chambron, J.-C.; Sauvage, J.-P. *J. Chem. Soc., Dalton Trans.* **1990**, 1841.
- (26) Nakai, H. *Bull. Chem. Soc. Jpn.* **1971**, *44*, 2412.
- (27) Foley, J.; Kenefick, D.; Phelan, D.; Tyagi, S.; Hathaway, B. *J. Chem. Soc., Dalton Trans.* **1983**, 2333.
- (28) Chia, L. M. D.; Radojevic, S.; Scowen, I. J.; McPartlin, M.; Halcrow, M. A. *Dalton* **2000**, 133.



ates Inc. Lewis-coil force magnetometer using  $\text{Hg}[\text{Co}(\text{NCS})_4]$  as a standard. Experimental susceptibility data were corrected for diamagnetic contributions. Electrochemical measurements were made at 25 °C on a EG&G PAR Model 253 Versa Stat potentiostat/galvanostat with electrochemical analysis software 270 for voltammetric work using a three electrode setup comprising a glassy carbon working electrode, platinum wire auxiliary electrode, and a saturated calomel reference (SCE) electrode. The electrochemical data were uncorrected for junction potentials. Tetrabutylammonium perchlorate (TBAP) and KCl were used as supporting electrolytes in nonaqueous and aqueous solvents, respectively.

**Preparation of  $[\text{Cu}(\text{Tp}^{\text{Ph}})(\text{L})](\text{ClO}_4)$  ( $\text{L} = \text{bpy}$ , **1**; **phen**, **2**; **dppq**, **3**; **dppz**, **4**).** Complexes **1–4** were prepared by following a general procedure. A 480 mg (1.0 mmol) quantity of  $\text{K}[\text{Tp}^{\text{Ph}}]$  was stirred with 200 mg (0.5 mmol) of dimeric copper(II) acetate·hydrate in 5 mL of  $\text{CH}_2\text{Cl}_2$  for 10 min. To this solution was added the heterocyclic base (1.0 mmol) dissolved in 5 mL of  $\text{CH}_2\text{Cl}_2$ . The mixture was stirred for 15 min followed by an addition of 2 mL of methanolic solution of sodium perchlorate (135 mg, 1.1 mmol). Stirring for a period of 7 h at 25 °C gave a blue-green solution which was reduced to a volume of ~2 mL by rotary evaporation. An addition of 20 mL of hexane followed by an overnight storage of the solution at -40 °C gave a green solid (yield: ~70%). The product was isolated, washed with hexane, and finally dried in vacuo over  $\text{P}_4\text{O}_{10}$ . Crystals of **1–4**, suitable for X-ray diffraction, were grown by slow diffusion of hexane into the  $\text{CH}_2\text{Cl}_2$  solution of the complex. Anal. Calcd for  $\text{C}_{37}\text{H}_{32}\text{N}_8\text{BClO}_5\text{Cu}(\mathbf{1}\cdot\text{H}_2\text{O})$ : C, 57.03; H, 4.11; N, 14.39. Found: C, 56.81; H, 4.23; N, 14.18. Anal. Calcd for  $\text{C}_{39}\text{H}_{30}\text{N}_8\text{BClO}_4\text{Cu}(\mathbf{2})$ : C, 59.69; H, 3.83; N, 14.28. Found: C, 59.39; H, 3.91; N, 14.18. Anal. Calcd for  $\text{C}_{41}\text{H}_{30}\text{N}_{10}\text{BClO}_4\text{Cu}(\mathbf{3})$ : C, 58.81; H, 3.59; N, 16.74. Found: C, 58.72; H, 3.65; N, 16.55. Anal. Calcd for  $\text{C}_{45}\text{H}_{32}\text{N}_{10}\text{BClO}_4\text{Cu}(\mathbf{4})$ : C, 60.91; H, 3.61; N, 15.80. Found: C, 60.79; H, 3.72; N, 15.62. **Caution!** Perchlorate salts are potentially explosive and should be handled in small quantities with care. The complexes are soluble in  $\text{CH}_2\text{Cl}_2$ , moderately soluble in acetonitrile, and sparingly soluble in methanol and water.

**X-ray Crystallographic Procedures.** The crystal structures of  $[\text{Cu}(\text{Tp}^{\text{Ph}})(\text{bpy})](\text{ClO}_4)\cdot\text{CH}_2\text{Cl}_2\cdot\text{H}_2\text{O}$ ,  $[\text{Cu}(\text{Tp}^{\text{Ph}})(\text{phen})](\text{ClO}_4)\cdot\text{CH}_2\text{Cl}_2$ ,  $[\text{Cu}(\text{Tp}^{\text{Ph}})(\text{dppq})](\text{ClO}_4)\cdot\text{CH}_2\text{Cl}_2$ , and  $[\text{Cu}(\text{Tp}^{\text{Ph}})(\text{dppz})](\text{ClO}_4)$  were obtained by single-crystal X-ray diffraction technique. Crystal mounting was done on glass fiber with epoxy cement. All geometric and intensity data were collected at room temperature using an automated Enraf–Nonius CAD4 diffractometer equipped with  $\text{Mo K}\alpha$  radiation ( $\lambda = 0.71073 \text{ \AA}$ ). Intensity data, collected using  $\omega$  scan mode, were corrected for Lorentz and polarization effects and for absorption. The structures were solved by the combination of Patterson and Fourier techniques and refined by full-matrix least-squares method using SHELX program.<sup>29</sup>

Complexes **1–3** crystallized with one  $\text{CH}_2\text{Cl}_2$  molecule as a solvent of crystallization. While the carbon atom of this solvent molecule refined well in all these structures, the chlorine atoms showed positional disorder. The difference Fourier map for **1** showed five peaks for the two chlorine atoms of  $\text{CH}_2\text{Cl}_2$ . While one chloride was positionally disordered to two peaks each with a site occupancy of 0.5, there were three peaks for the other chloride atom. These peaks were refined with a site occupancy of 0.5, 0.25, and 0.25. In structure **2**, the perchlorate anion was found to be positionally disordered. While two oxygen atoms were refined well with a site occupancy factor (SOF) of 1.0, four peaks were located

each with a SOF value of 0.5 for the other two oxygen atoms. The chloride atoms of lattice  $\text{CH}_2\text{Cl}_2$  in **2** were found to be severely disordered. There were six peaks for one chloride atom. One peak was refined with a SOF value of 0.5; the rest were refined with a SOF value of 0.1. The second chloride atom comprised five peaks. Three of them refined with SOF 0.2, one with 0.3, and the fifth with 0.1. In **3**, only one chloride of  $\text{CH}_2\text{Cl}_2$  was found to be positionally disordered. Two peaks with a SOF value of 0.3 and 0.7 were refined. Structure **4** did not have a lattice solvent molecule. Complex **1** also showed the presence of one water molecule as a solvent of crystallization.

All hydrogen atoms belonging to the complex cation in **1** and **2** except one hydrogen of bpy were located from the difference Fourier map and refined. The BH hydrogen in **3** and **4** was located from the Fourier map. The remaining hydrogen atoms of **3** and **4** and the bpy hydrogen atom, other than the solvent molecules, were in fixed position and refined using a riding model. All non-hydrogen atoms, except those positionally disordered ones, were refined anisotropically. Total reflections, data with  $I > 2\sigma(I)$ , and parameters refined for **1–4** were 6574, 3779, 623; 7033, 4631, 658; 3758, 2646, 553; and 3987, 2973, 563, respectively. The goodness-of-fit and the largest difference peak for **1–4** are 0.997, 0.661; 1.062, 0.625; 1.013, 0.373; and 1.036, 0.394, respectively. The higher residual (*R*) values for the bpy and phen structures could be due to the presence of disordered solvent molecules. Such disorder, however, had no significant impact on the structural parameters of the complexes. Selected crystal data for the complexes are summarized in Table 1. Perspective views of the molecules were obtained by ORTEP.<sup>30</sup>

**DNA Binding and Cleavage Experiments.**<sup>31a</sup> The concentration of CT DNA was determined from the absorption intensity at 260 nm with a known  $\epsilon$  value of  $6600 \text{ M}^{-1} \text{ cm}^{-1}$ .<sup>31b</sup> Relative binding of complexes **1–4** to CT DNA with respect to the bis-phen copper(II) complex was studied by fluorescence spectral method using ethidium bromide (EB) bound CT DNA solution in Tris-HCl/NaCl buffer (pH 7.2). The fluorescence intensities at 601 nm (510 nm excitation) of EB with an increasing amount of the complex concentration were recorded. The cleavage of DNA was monitored by agarose gel electrophoresis. Supercoiled pUC19 DNA (6  $\mu\text{L}$ , ~500 ng) in 50 mM Tris-HCl buffer (pH, 7.2) containing 50 mM NaCl was treated with the metal complex (65  $\mu\text{M}$ ) and ascorbic acid ( $\text{H}_2\text{A}$ , 250  $\mu\text{M}$ ) followed by dilution with the Tris-HCl buffer to a total volume of 20  $\mu\text{L}$ . The samples after incubation for 1 h at 37 °C were added to the loading buffer containing 25% bromophenol blue, 0.25% xylene cyanol, and 30% glycerol (3  $\mu\text{L}$ ), and the solution was finally loaded on 0.8% agarose gel containing 1.0  $\mu\text{g}/\text{mL}$  EB. Electrophoresis was carried out for 3 h at 40 V in TBE buffer. Bands were visualized by UV light and photographed. The extent of DNA cleavage was measured from the intensities of the bands using BIORAD Gel Documentation System. Due correction was made for the low level of nicked circular (NC) form present in the original supercoiled (SC) DNA sample and for the low affinity of EB binding to SC compared to NC and linear forms of DNA.<sup>23</sup> In the inhibition reactions, distamycin (75  $\mu\text{M}$ ) or DMSO (4  $\mu\text{L}$ ) was added initially to pUC19 DNA (~500 ng) in 50 mM Tris-HCl/NaCl buffer, and incubation was done for 15 min at 37 °C prior to the addition of the ternary complexes (**2–4**, 70  $\mu\text{M}$ )

(30) Johnson, C. K. ORTEP; Report ORNL-5138; Oak Ridge National Laboratory: Oak Ridge, TN, 1976.

(31) (a) Abbreviations used: CT, calf thymus; SC, supercoiled; NC, nicked circular; EB, ethidium bromide;  $\text{H}_2\text{A}$ , ascorbic acid. (b) Reichmann, M. E.; Rice, S. A.; Thomas, C. A.; Doty, P. *J. Am. Chem. Soc.* **1954**, *76*, 3047.

(29) Sheldrick, G. M. *SHELX-97, Programs for Crystal Structure Solution and Refinement*; University of Göttingen: Göttingen, Germany, 1997.

**Table 1.** Selected Crystallographic Data for the Complexes [Cu(Tp<sup>Ph</sup>)(L)](ClO<sub>4</sub>) [L = bpy, **1**; phen, **2**; dpq, **3**; dppz, **4**]

	1·CH <sub>2</sub> Cl <sub>2</sub> ·H <sub>2</sub> O	2·CH <sub>2</sub> Cl <sub>2</sub>	3·CH <sub>2</sub> Cl <sub>2</sub>	4
formula	C <sub>38</sub> H <sub>34</sub> BCuCl <sub>3</sub> N <sub>8</sub> O <sub>5</sub>	C <sub>40</sub> H <sub>32</sub> BCuCl <sub>3</sub> N <sub>8</sub> O <sub>4</sub>	C <sub>42</sub> H <sub>32</sub> BCuCl <sub>3</sub> N <sub>10</sub> O <sub>4</sub>	C <sub>45</sub> H <sub>32</sub> BCuClN <sub>10</sub> O <sub>4</sub>
fw, g mol <sup>-1</sup>	863.43	869.44	921.48	886.61
space group (No.)	P2 <sub>1</sub> /n (1014)	P2 <sub>1</sub> /n (1014)	Cc (9)	P2 <sub>1</sub> 2 <sub>1</sub> 2 <sub>1</sub> (19)
a, Å	11.111(7)	11.362(4)	22.107(5)	12.661 (5)
b, Å	30.197(5)	30.295(9)	13.219(2)	16.017 (4)
c, Å	11.527(3)	11.672(3)	14.493(5)	20.078 (7)
α, deg	90.0	90.0	90.0	90.0
β, deg	94.42(3)	95.46(2)	100.92(2)	90.0
γ, deg	90.0	90.0	90.0	90.0
V, Å <sup>3</sup>	3856(3)	3999(2)	4159(2)	4072(2)
Z	4	4	4	4
T, K	293(2)	293(2)	293(2)	293(2)
ρ <sub>calcd</sub> , g cm <sup>-3</sup>	1.487	1.444	1.472	1.446
λ, Å (Mo Kα)	0.71073	0.71073	0.71073	0.71073
μ, cm <sup>-1</sup>	8.30	7.99	7.74	6.61
R (F <sub>o</sub> ) <sup>a</sup> [R all data]	0.0736[0.1269]	0.0571 [0.0941]	0.0448 [0.0752]	0.0402 [0.0620]
wR (F <sub>o</sub> ) <sup>b</sup> [wR (all data)]	0.1892 [0.2185]	0.1549 [0.1735]	0.1009 [0.1132]	0.0962 [0.1071]

<sup>a</sup> R = Σ||F<sub>o</sub> - |F<sub>c</sub>||/Σ|F<sub>o</sub>|. <sup>b</sup> wR = [Σw(|F<sub>o</sub> - |F<sub>c</sub>||)<sup>2</sup>/Σw|F<sub>o</sub>|<sup>2</sup>]<sup>1/2</sup>, where w = 1/[σ<sup>2</sup>(F<sub>o</sub>) + (AP)<sup>2</sup> + BP] where ρ = [max(F<sub>o</sub><sup>2</sup>, 0) + 2F<sub>c</sub><sup>2</sup>]/3. A and B values are 0.1319 and 0.0 for **1**, 0.0966 and 1.7142 for **2**, 0.0631 and 0.0 for **3**, and 0.0575 and 1.0344 for **4**.

**Table 2.** Selected IR, Vis, and EPR Spectral Data for [Cu(Tp<sup>Ph</sup>)(L)](ClO<sub>4</sub>) (**1–4**)

complex	IR <sup>a</sup> , cm <sup>-1</sup>		λ, nm (ε, M <sup>-1</sup> cm <sup>-1</sup> ) <sup>b</sup>	EPR <sup>c</sup>	
	ν <sub>B-H</sub>	ν <sub>ClO<sub>4</sub></sub>		g <sub>  </sub> (A <sub>  </sub> , G)	g <sub>⊥</sub>
[Cu(Tp <sup>Ph</sup> (bpy))](ClO <sub>4</sub> ) ( <b>1</b> )	2518	1088	632 (130)	2.17 (128)	2.07
[Cu(Tp <sup>Ph</sup> (phen))](ClO <sub>4</sub> ) ( <b>2</b> )	2532	1088	654 (74)	2.17 (128)	2.07
[Cu(Tp <sup>Ph</sup> (dpq))](ClO <sub>4</sub> ) ( <b>3</b> )	2485	1088	648 (82)	2.19 (128)	2.07
[Cu(Tp <sup>Ph</sup> (dppz))](ClO <sub>4</sub> ) ( <b>4</b> )	2470	1088	655 (97)	2.18 (128)	2.07

<sup>a</sup> In KBr phase. <sup>b</sup> In CH<sub>2</sub>Cl<sub>2</sub>. <sup>c</sup> In CH<sub>2</sub>Cl<sub>2</sub> glass at 77 K.

and H<sub>2</sub>A (250 μM). The mixture was diluted with the buffer to a total volume of 20 μL. After a further incubation of 1 h at 37 °C, the samples were subjected for gel electrophoresis using the described procedures.

## Results and Discussion

**Synthesis and General Aspects.** The complexes have been prepared in high yield from a reaction of [Cu<sub>2</sub>(O<sub>2</sub>CMe)<sub>4</sub>(H<sub>2</sub>O)<sub>2</sub>] with the potassium salt of tris(3-phenylpyrazolyl)-borate and the heterocyclic base (L) and are isolated as perchlorate salts. A phenyl substitution at the 3-position of the pyrazolyl ring is found to be an essential requirement to stabilize the ternary complex. The unsubstituted tris(pyrazolyl)borate, under similar reaction conditions, has led to the formation of the bis-chelates of Tp and the bis-chelate of the N,N-donor base (L). Complexes **1–4** are 1:1 electrolytic and are stable in the solid as well as in a solution phase. The complexes are formulated as [Cu(Tp<sup>Ph</sup>)(L)](ClO<sub>4</sub>) (**1–4**) from the elemental analysis data. Selected spectral data are given in Table 2.

The formation of the cationic complex with Tp<sup>Ph</sup> ligand is evidenced from the presence of a perchlorate stretch at 1088 cm<sup>-1</sup> and a B–H stretch near 2500 cm<sup>-1</sup> in the infrared spectra of the complexes. The B–H stretch, which appears at 2411 cm<sup>-1</sup> in K[TP<sup>Ph</sup>],<sup>22</sup> shifts to higher energy in **1–4**. A similar shift has previously been reported in Tp complexes of transition metals.<sup>32</sup> Complexes **2–4**, having planar heterocyclic bases, show a systematic variation of the B–H

stretching frequency as dppz < dpq < phen. This could be related to their π-acidity.

The complexes are one-electron paramagnetic species giving a μ value of ca. 1.8 μ<sub>B</sub>. The EPR spectra of **1–4** in CH<sub>2</sub>Cl<sub>2</sub> glass at 77 K show axial symmetry with g<sub>||</sub> > g<sub>⊥</sub> indicating the copper in a {d<sub>x<sup>2</sup>-y<sup>2</sup></sub>}<sup>1</sup> ground state. The g<sub>||</sub> and g<sub>⊥</sub> values are essentially similar in all four complexes. The A<sub>||</sub> value of 128 G is, however, significantly lower than the A<sub>||</sub> value of ca. 170 G observed in related ternary copper(II) species having square-pyramidal geometry.<sup>28,32,33</sup> The smaller A<sub>||</sub> value suggests significant delocalization of the unpaired electron density on the metal to the N,N-donor heterocyclic ligand at the basal plane. The g<sub>||</sub> values reported by Halcrow and co-workers on analogous ternary square-pyramidal copper(II) complexes are ca. 2.28.<sup>33</sup> This value is significantly higher than the g<sub>||</sub> value of 2.18 observed in **1–4**. The EPR data indicate a distorted square-pyramidal geometry in **1–4**. The complexes display a broad d–d band in the visible electronic spectra near 650 nm in CH<sub>2</sub>Cl<sub>2</sub>.

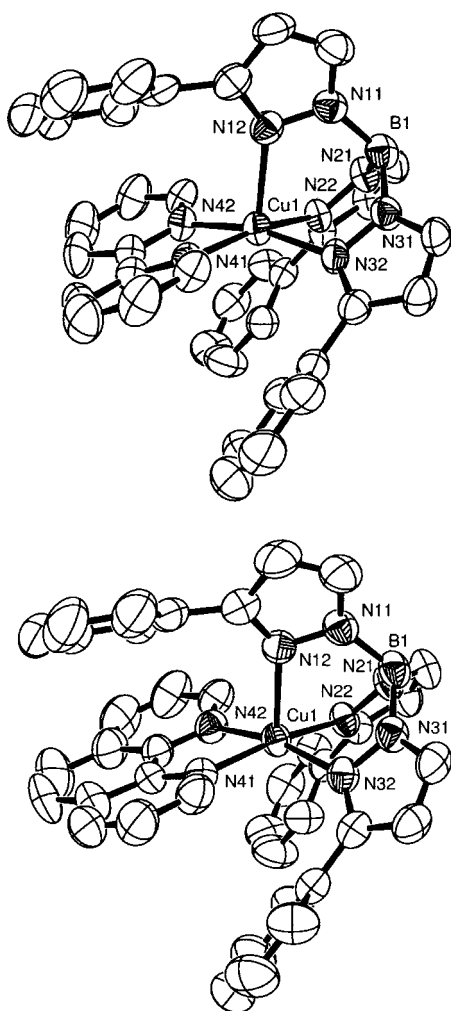
**Crystal Structures.** All the complexes are characterized by single-crystal X-ray diffraction technique. Selected bond distances and angles are given in Table 3. The structure of the cationic complex consists of a discrete monomeric species with the metal in a distorted square-pyramidal coordination geometry (Figures 1 and 2). The donor atoms in the basal plane are two nitrogen atoms from the heterocyclic base L and two nitrogen atoms from the Tp<sup>Ph</sup> ligand. The nitrogen of the third 3-phenylpyrazolyl ring is bonded at the apical site. The Cu–N (equatorial) and Cu–N (axial) distances are ~2.0 and 2.2 Å, respectively. The three phenyl groups of the Tp<sup>Ph</sup> anion in **1–4** form a bowl-shaped structure that sterically encloses the {CuL} moiety. The encumbrance effect is more for the bpy and phen species. The dpq and

(32) Perkinson, J.; Brodie, S.; Yoon, K.; Mosny, K.; Carroll, P. J.; Morgan, T. V.; Burgmayer, S. J. *N. Inorg. Chem.* **1991**, *30*, 719.

(33) (a) Halcrow, M. A.; Chia, L. M. L.; Liu, X.; McInnes, E. J. L.; Yellowlees, L. J.; Mabbs, F. E.; Scowen, I. J.; McPartlin, M.; Davies, J. E. *J. Chem. Soc., Dalton Trans.* **1999**, 1753. (b) Halcrow, M. A.; McInnes, E. J. L.; Mabbs, F. E.; Scowen, I. J.; McPartlin, M.; Powell, H. R.; Davies, J. E. *J. Chem. Soc., Dalton Trans.* **1997**, 4025. (c) Foster, C. L.; Liu, X.; Kilner, C. A.; Pett, M. T.; Halcrow, M. A. *Dalton* **2000**, 4563.

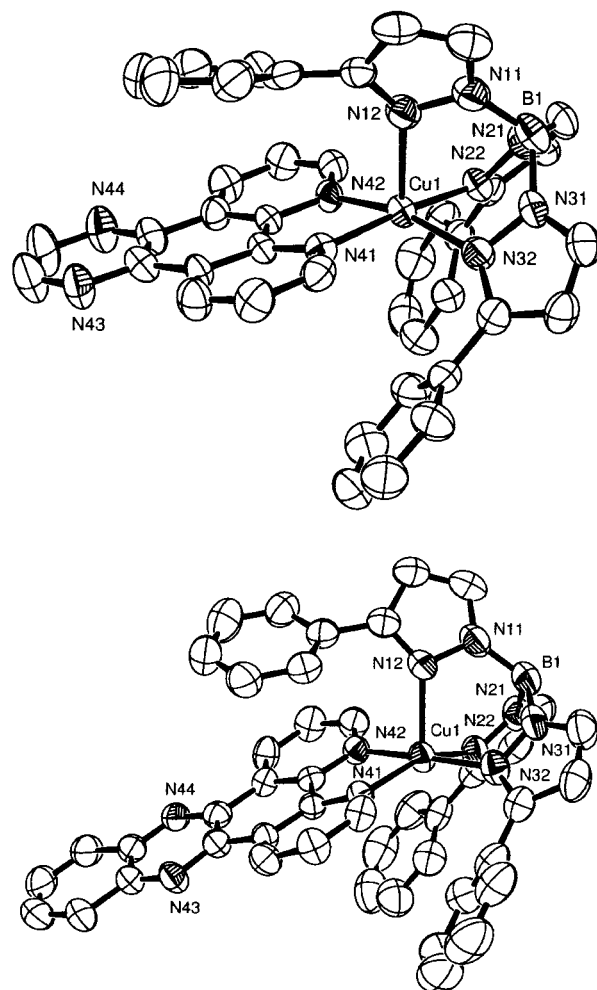
**Table 3.** Selected Bond Distances (Å) and Angles (deg) in [Cu(Tp<sup>Ph</sup>)(L)](ClO<sub>4</sub>) (L = bpy, **1**; phen, **2**; dpq, **3**; dppz, **4**) with Their Estimated Standard Deviations in Parentheses

	<b>1</b> ·CH <sub>2</sub> Cl <sub>2</sub> ·H <sub>2</sub> O	<b>2</b> ·CH <sub>2</sub> Cl <sub>2</sub>	<b>3</b> ·CH <sub>2</sub> Cl <sub>2</sub>	<b>4</b>
Cu(1)–N(12)	2.223(5)	2.236(3)	2.189(6)	2.186(4)
Cu(1)–N(22)	2.015(5)	2.013(3)	2.004(6)	2.006(5)
Cu(1)–N(32)	2.017(5)	2.018(3)	2.032(6)	2.037(5)
Cu(1)–N(41)	2.013(5)	2.022(4)	2.016(5)	2.032(4)
Cu(1)–N(42)	2.009(5)	2.034(3)	2.042(3)	2.027(4)
B(1)–H(1)	1.19(6)	1.04(5)	1.00(7)	1.15(5)
N(12)–Cu(1)–N(22)	93.7(2)	93.87(13)	92.7(2)	95.1(2)
N(12)–Cu(1)–N(32)	90.7(2)	91.12(14)	92.8(2)	90.1(2)
N(12)–Cu(1)–N(41)	98.7(2)	96.31(14)	93.9(3)	108.4(2)
N(12)–Cu(1)–N(42)	103.0(2)	102.47(14)	102.1(2)	92.3(2)
N(22)–Cu(1)–N(32)	85.7(2)	85.73(14)	84.5(2)	86.1(2)
N(22)–Cu(1)–N(41)	167.3(2)	169.70(14)	173.3(3)	155.5(2)
N(22)–Cu(1)–N(42)	94.8(2)	95.07(14)	97.1(2)	91.7(2)
N(32)–Cu(1)–N(41)	97.0(2)	95.64(14)	96.1(3)	100.7(2)
N(32)–Cu(1)–N(42)	166.3(2)	166.29(14)	164.9(2)	176.9(2)
N(41)–Cu(1)–N(42)	79.7(2)	81.19(14)	80.6(2)	80.5(2)

**Figure 1.** ORTEP views of the cationic complexes in [Cu(Tp<sup>Ph</sup>)(bpy)](ClO<sub>4</sub>)·CH<sub>2</sub>Cl<sub>2</sub>·H<sub>2</sub>O (**1**·CH<sub>2</sub>Cl<sub>2</sub>·H<sub>2</sub>O) (top) and [Cu(Tp<sup>Ph</sup>)(phen)](ClO<sub>4</sub>)·CH<sub>2</sub>Cl<sub>2</sub> (**2**·CH<sub>2</sub>Cl<sub>2</sub>) (bottom) showing the atom numbering scheme and 50% probability thermal ellipsoids. Carbon atoms are not labeled for clarity.

dppz complexes have the extended aromatic ring(s) stemmed outside the bowl.

The extent of distortion of the square-pyramidal coordination geometry can be estimated from the  $\tau$  value of 0.02 for **1**, 0.06 for **2**, 0.14 for **3**, and 0.35 for **4** ( $\tau = 0.0$  for idealized

**Figure 2.** ORTEP diagrams of the complex cation in [Cu(Tp<sup>Ph</sup>)(dpq)](ClO<sub>4</sub>)·CH<sub>2</sub>Cl<sub>2</sub> (**3**·CH<sub>2</sub>Cl<sub>2</sub>) (top) and [Cu(Tp<sup>Ph</sup>)(dppz)](ClO<sub>4</sub>) (**4**) (bottom) with the atom numbering of the metal and heteroatoms showing the thermal ellipsoids at 50% probability level.

square-pyramidal and 1.0 for trigonal-bipyramidal geometry).<sup>34</sup> While the bpy and phen complexes are essentially square-pyramidal, the dpq and dppz complexes show major distortion. The bite angle N(41)–Cu(1)–N(42) is essentially same for **1**–**4**. A major deviation is observed in the N(22)–Cu(1)–N(41) and N(32)–Cu(1)–N(42) angles. This could be due to the planar structure of phen, dpq, and dppz ligands. The tetragonal distortion involving the Cu(1)–N(12) bond is found to be less in **3** and **4** compared to that in **1** and **2**.

**Electrochemistry.** The complexes are redox-active and display quasireversible cyclic voltammetric responses for the Cu(II)/Cu(I) couple near 0.0 V versus SCE with an  $i_{pc}/i_{pa}$  ratio of unity in CH<sub>2</sub>Cl<sub>2</sub> or DMF (Table 4; Figure 3). The  $E_{1/2}$  values suggest the stability order for the copper(I) species as **4** (dppz) > **3** (dpq) > **2** (phen) > **1** (bpy). A greater stabilization of the Cu(I) species for the dppz complex is related to the presence of the phenazine moiety enhancing the  $\pi$ -acidity of the ligand. The reduced species is unstable in MeCN and aqueous medium giving a higher  $i_{pc}/i_{pa}$  ratio. The complexes in Tris-HCl buffer (pH 7.2) display only the

(34) Addison, A. W.; Rao, T. N.; Reedijk, J.; Rijn, J. V.; Verschoor, G. C. *J. Chem. Soc., Dalton Trans.* **1984**, 1349.



**Table 4.** Cyclic Voltammetric Data<sup>a</sup> for Complexes 1–4

complex	solvent <sup>b</sup>	$E_{1/2}$ , V ( $\Delta E_p$ , mV)	$i_{pc}/i_{pa}$
[Cu(Tp <sup>Ph</sup> )(bpy)](ClO <sub>4</sub> ) (1)	CH <sub>2</sub> Cl <sub>2</sub>	-0.039 (145)	1.04
	MeCN	-0.034 <sup>c</sup>	2.60
	DMF	0.053 (100)	1.09
	H <sub>2</sub> O–DMF (1:1)	-0.014 (145)	
[Cu(Tp <sup>Ph</sup> )(phen)](ClO <sub>4</sub> ) (2)	CH <sub>2</sub> Cl <sub>2</sub>	-0.021 (145)	1.03
	MeCN	-0.020 (108)	1.34
	DMF	0.059 (115)	1.04
	H <sub>2</sub> O–DMF (1:1)	-0.013 (145)	0.62
[Cu(Tp <sup>Ph</sup> )(dpq)](ClO <sub>4</sub> ) (3)	CH <sub>2</sub> Cl <sub>2</sub>	0.034 (155)	1.00
	MeCN	0.028 (190)	1.50
	DMF	0.084 (150)	1.02
	H <sub>2</sub> O–DMF (1:1)	-0.006 <sup>d</sup>	
[Cu(Tp <sup>Ph</sup> )(dppz)](ClO <sub>4</sub> ) (4)	CH <sub>2</sub> Cl <sub>2</sub>	0.036 (155)	1.02
	MeCN	0.037 (170)	1.45
	DMF	0.086 (130)	1.05
	H <sub>2</sub> O–DMF (1:1)	0.034 <sup>e</sup>	

<sup>a</sup> Scan rate, 50 mV s<sup>-1</sup>. Potentials are versus SCE.  $E_{1/2} = 0.5(E_{pa} + E_{pc})$ .  $\Delta E_p = E_{pa} - E_{pc}$ .  $i_{pa}$  and  $i_{pc}$  are anodic and cathodic peak currents, respectively. <sup>b</sup> Supporting electrolyte: 0.1 M TBAP for nonaqueous and 0.1 M KCl for aqueous medium. <sup>c</sup> Cathodic peak potential ( $E_{pc}$ ) with a broad anodic response ( $E_{pa}$ ) at 0.11 V. <sup>d</sup>  $E_{pc}$  with very weak anodic response at 0.44 V. <sup>e</sup>  $E_{pc}$  value with weak anodic peaks at 0.17 (broad) and 0.52 V.

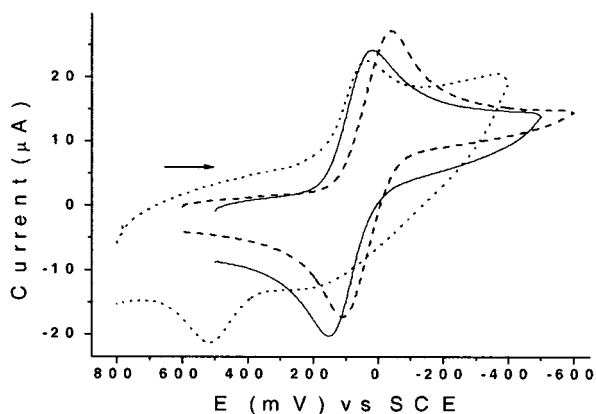


**Figure 3.** Cyclic voltammograms of [Cu(Tp<sup>Ph</sup>)(dppz)](ClO<sub>4</sub>) (4) in CH<sub>2</sub>Cl<sub>2</sub>–0.1 M TBAP (---), DMF–0.1 M TBAP (–), and DMF–H<sub>2</sub>O(1:1 v/v)–0.1 M KCl (···) at 50 mV s<sup>-1</sup>.

cathodic peak with no visible anodic counterpart. In addition to the Cu(II)/Cu(I) couple, the dppz and dpq complexes show a one-electron quasireversible reduction process at -1.19 V ( $\Delta E_p = 152$  mV) and -1.40 V ( $\Delta E_p = 100$  mV), respectively, in CH<sub>2</sub>Cl<sub>2</sub>–0.1 M TBAP at 50 mV s<sup>-1</sup> involving the planar heterocyclic base.<sup>35</sup>

**DNA Binding and Cleavage.** The binding of 1–4, [Cu(Tp<sup>Ph</sup>)(O<sub>2</sub>CMe)], and [Cu(phen)<sub>2</sub>(H<sub>2</sub>O)](ClO<sub>4</sub>)<sub>2</sub> to the calf thymus DNA has been studied by fluorescence spectral method. Ethidium bromide (EB) bound to DNA shows enhanced emission intensity compared to the free EB. A competitive binding of the complex to CT DNA causes displacement of bound EB, and as a result, the emission intensity reduces because of fluorescence quenching of the free EB by the solvent molecules. The decrease in emission intensity at different complex concentrations is shown in Figure 4a. The monocationic complexes 2–4 show similar

(35) When the cathodic scan is made up to -1.8 V in CH<sub>2</sub>Cl<sub>2</sub>–0.1 M TBAP, a weak and irreversible anodic peak, in addition to the Cu(II)/Cu(I) couple and the ligand reduction process, is observed at 0.49 V for 3 and 0.75 V for 4. This peak is, however, absent in the potential scan limit of 1.0 to -1.0 V.

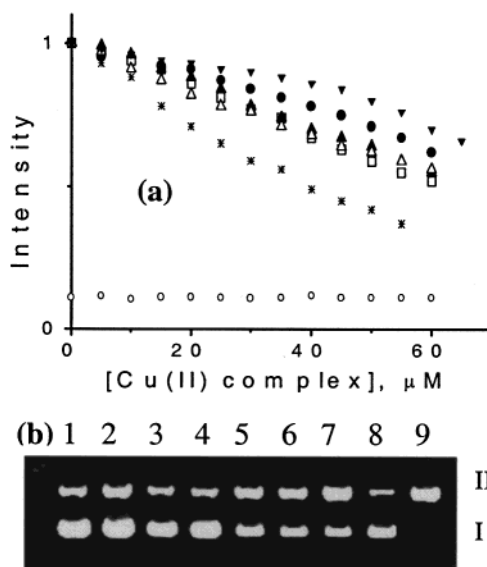


**Figure 4.** (a) Effect of addition of [Cu(Tp<sup>Ph</sup>)(L)](ClO<sub>4</sub>) (L = bpy, 1, ●; phen, 2, □; dpq, 3, ▲; dppz, 4, △), [Cu(Tp<sup>Ph</sup>)(O<sub>2</sub>CMe)] (▼), and [Cu(phen)<sub>2</sub>(H<sub>2</sub>O)](ClO<sub>4</sub>)<sub>2</sub> (\*) to the emission intensity of the 125 µM CT DNA-bound ethidium bromide (12.5 µM) at different complex concentrations (0–65 µM) in a 5 mM Tris-HCl/50 mM NaCl buffer (pH 7.2) containing 1% DMF at 25 °C. The emission intensities of EB (in the absence of DNA) at various concentrations of complex 3 are also shown (○). (b) Cleavage of supercoiled pUC19 DNA (0.5 µg) by [Cu(Tp<sup>Ph</sup>)(L)](ClO<sub>4</sub>) (1–4) and the reference complexes [Cu(Tp<sup>Ph</sup>)(O<sub>2</sub>CMe)] and [Cu(phen)<sub>2</sub>(H<sub>2</sub>O)](ClO<sub>4</sub>)<sub>2</sub> in the presence of ascorbic acid (H<sub>2</sub>A, 250 µM) in a 50 mM Tris-HCl/NaCl buffer at 37 °C containing DMF (10%). Lane 1, DNA control; lane 2, DNA + H<sub>2</sub>A; lane 3, DNA + complex 3; lanes 4–7, DNA + H<sub>2</sub>A + complexes 1–4, respectively; lane 8, DNA + H<sub>2</sub>A + [Cu(Tp<sup>Ph</sup>)(O<sub>2</sub>CMe)]; lane 9, DNA + H<sub>2</sub>A + [Cu(phen)<sub>2</sub>(H<sub>2</sub>O)](ClO<sub>4</sub>)<sub>2</sub>. Complex concentration was 65 µM. Forms I and II are supercoiled and nicked circular, respectively.

slopes indicating similar binding propensity to CT DNA. The binding is, however, lower than that observed for the dicationic bis(phen)Cu(II) species. The tris(3-phenylpyrazolyl)borate copper(II) complex in absence of the planar heterocyclic base does not show any significant binding. The same is true for bpy complex 1. Binding of the complexes to DNA follows the order Cu(phen)<sub>2</sub><sup>2+</sup> > 4 ~ 3 ~ 2 > 1 > Cu(Tp<sup>Ph</sup>)(O<sub>2</sub>CMe). It is evident that the steric encumbrance caused by the phenyl groups of Tp<sup>Ph</sup> reduces the intercalative mode of binding of the planar heterocyclic bases in complexes 2–4.

The nuclease activity of the complexes has been studied using supercoiled pUC19 DNA in a medium of Tris-HCl/NaCl buffer in the presence of ascorbic acid as a reducing agent. The extent of cleavage of SC DNA has been determined by gel electrophoresis on the basis of the conversion of the SC to NC DNA form (Table 5, Figure 4b). While complexes 1 and [Cu(Tp<sup>Ph</sup>)(O<sub>2</sub>CMe)] are cleavage inactive, complexes 2–4 show moderate cleavage giving the order [Cu(phen)<sub>2</sub>(H<sub>2</sub>O)](ClO<sub>4</sub>)<sub>2</sub> > [Cu(Tp<sup>Ph</sup>)(dppz)](ClO<sub>4</sub>) (4) > [Cu(Tp<sup>Ph</sup>)(dpq)](ClO<sub>4</sub>) (3) ~ [Cu(Tp<sup>Ph</sup>)(phen)](ClO<sub>4</sub>) (2). The steric encumbrance of the Tp<sup>Ph</sup> ligand is clearly evidenced in the conversion of the SC to the NC form. The dppz complex with its protruding phenazine ring can effectively intercalate and cleave DNA mediated by a Cu(II)/Cu(I) redox couple in the presence of ascorbic acid and dioxygen.



**Table 5.** Comparison of the pUC19 DNA Cleavage Efficiency of Complexes 1–4 along with Two Reference Copper(II) Complexes in Presence of Ascorbic Acid (H<sub>2</sub>A)

serial no. <sup>a</sup>	reaction condition <sup>b</sup>	form %	
		SC <sup>c</sup>	NC <sup>c</sup>
1	DNA Control	85	15
2	DNA + H <sub>2</sub> A	78	22
3	DNA + [Cu(Tp <sup>Ph</sup> )(dpq)](ClO <sub>4</sub> ) (3)	86	14
4	DNA + H <sub>2</sub> A + [Cu(Tp <sup>Ph</sup> )(bpy)](ClO <sub>4</sub> ) (1)	85	15
5	DNA + H <sub>2</sub> A + [Cu(Tp <sup>Ph</sup> )(phen)](ClO <sub>4</sub> ) (2)	59	41
6	DNA + H <sub>2</sub> A + [Cu(Tp <sup>Ph</sup> )(dpq)](ClO <sub>4</sub> ) (3)	58	42
7	DNA + H <sub>2</sub> A + [Cu(Tp <sup>Ph</sup> )(dppz)](ClO <sub>4</sub> ) (4)	39	61
8	DNA + H <sub>2</sub> A + [Cu(Tp <sup>Ph</sup> )(O <sub>2</sub> CMe)]	90	10
9	DNA + H <sub>2</sub> A + [Cu(phen) <sub>2</sub> (H <sub>2</sub> O)](ClO <sub>4</sub> ) <sub>2</sub>	5	95

<sup>a</sup> The serial number is the same as the lane number shown in Figure 4b.

<sup>b</sup> Concentrations of different species are given in the Experimental Section.

<sup>c</sup> SC and NC are supercoiled and nicked circular forms, respectively.

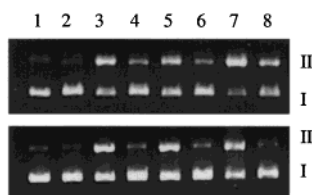


**Figure 5.** Gel electrophoresis diagrams for the cleavage of pUC19 DNA with complexes 2–4 and ascorbic acid in a Tris-HCl/NaCl buffer (pH 7.2) at 37 °C using inhibitors distamycin (top) and DMSO (bottom). Lane 1, DNA control; lane 2, DNA + distamycin (top) and DNA + DMSO (bottom); lane 3, complex 2 + H<sub>2</sub>A + DNA; lane 4, complex 2 + H<sub>2</sub>A + DNA + distamycin (top) or DMSO (bottom); lane 5, complex 3 + H<sub>2</sub>A + DNA; lane 6, complex 3 + H<sub>2</sub>A + distamycin (top) or DMSO (bottom); lane 7, complex 4 + H<sub>2</sub>A + DNA; lane 8, complex 4 + H<sub>2</sub>A + DNA + distamycin (top) or DMSO (bottom). Forms I and II are SC and NC DNA, respectively. In the inhibition reactions, distamycin or DMSO was incubated with SC DNA prior to the addition of the complex and the reducing agent ascorbic acid (H<sub>2</sub>A).

The mechanistic aspects of the DNA binding and cleavage reactions involving [Cu(Tp<sup>Ph</sup>)(L)]<sup>+</sup> complexes 2–4 have been investigated using inhibiting reagents such as DMSO and distamycin. It has earlier been postulated that Cu(phen)<sub>2</sub><sup>+</sup> binds at the minor groove of B-DNA and the DNA cleavage results from H-1' abstraction by an oxidizing species. In the B-DNA helix, the deoxy ribose hydrogen H-1' is accessible to the minor-groove binding molecules such as the bis(phen)-copper complex. The mechanistic pathway involving the H-1' proton abstraction has been suggested by Sigman and co-workers from the isolation of a cleavage product 5-methylene-2-furanone (MF).<sup>36</sup> To probe the groove-binding preferences of complexes 2–4, we have used the minor-groove binder distamycin as an inhibition reagent in the cleavage reactions. Incubation of SC pUC19 DNA with distamycin prior to the addition of complexes 2–4 and ascorbic acid (H<sub>2</sub>A), and subsequent gel electrophoresis, shows a complete inhibition for [Cu(Tp<sup>Ph</sup>)(phen)]<sup>+</sup> and [Cu(Tp<sup>Ph</sup>)(dpq)]<sup>+</sup>, while [Cu(Tp<sup>Ph</sup>)(dppz)]<sup>+</sup> exhibits significant DNA cleavage (Figure 5). This suggests a minor groove preference for the phen and dpq complexes and a major groove binding for the dppz complex.<sup>36–38</sup> An abstraction of 3'-hydrogen which is located in the major groove is likely to be a plausible mechanistic pathway for the cleavage reactions involving the dppz

(36) Meijler, M. M.; Zelenko, O.; Sigman, D. S. *J. Am. Chem. Soc.* **1997**, *119*, 1135.

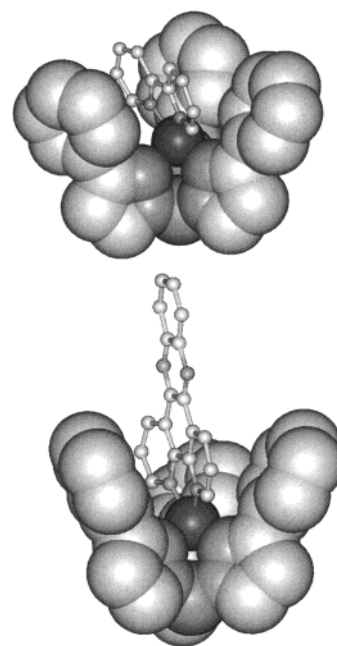


**Figure 6.** Molecular models for the bpy complex 1 (top) and the dppz complex 4 (bottom) displaying the steric encumbrance caused by the three phenyl groups of the Tp<sup>Ph</sup> ligand to the {CuL} moiety.

species. The results are of significance as the majority of the oxidative cleavage reagents generally bind in the minor groove rather than the major groove.<sup>16</sup> The photoactive octahedral metallointercalators of rhodium and ruthenium are known to cleave B-DNA by H-3' abstraction pathway through major groove binding.<sup>38</sup> Complex 4 exemplifies a copper based “chemical nuclease” showing major groove binding preference.

The redox-active copper complexes in the presence of a reducing agent cleave nucleic acids by oxidative attack at the sugar moiety. The true identity of the oxidizing species is yet to be conclusively established. It could be either free hydroxyl radical or a copper(III) bound oxo or hydroxo species.<sup>39,40</sup> We have probed the DNA strand scission using complexes 2–4 in the presence of ascorbic acid and a hydroxyl radical scavenger like DMSO. The gel electrophoresis diagram, which shows a complete inhibition of DNA cleavage in the presence of DMSO, suggests the involvement of hydroxyl radical in the scission reactions (Figure 5). In summary, the DNA binding studies show the formation of a [Cu<sup>II</sup>(Tp<sup>Ph</sup>)(L)]<sup>+</sup>···DNA adduct which undergoes reduction with ascorbic acid (H<sub>2</sub>A) to form [Cu<sup>I</sup>(Tp<sup>Ph</sup>)(L)]···DNA in

(37) (a) Collins, J. G.; Sleeman, A. D.; Aldrich-Wright, J. R.; Greguric, I.; Hambley, T. W. *Inorg. Chem.* **1998**, *37*, 3133. (b) Fry, J. V.; Collins, J. G. *Inorg. Chem.* **1997**, *36*, 2919. (c) Greguric, I.; Aldrich-Wright, J. R.; Collins, J. G. *J. Am. Chem. Soc.* **1997**, *119*, 3621.

(38) (a) Erkkila, K. E.; Odom, D. T.; Barton, J. K. *Chem. Rev.* **1999**, *99*, 2777. (b) Holmlin, R. E.; Stemp, E. D. A.; Barton, J. K. *Inorg. Chem.* **1998**, *37*, 29. (c) Dupureur, C. M.; Barton, J. K. *Inorg. Chem.* **1997**, *36*, 33. (d) Dupureur, C. M.; Barton, J. K. *J. Am. Chem. Soc.* **1994**, *116*, 10286. (e) Sitlani, A.; Long, E. C.; Pyle, A. M.; Barton, J. K. *J. Am. Chem. Soc.* **1992**, *114*, 2302.

(39) (a) Que, B. G.; Downey, K. M.; So, A. G. *Biochemistry* **1980**, *19*, 5987. (b) Graham, D. R.; Marshall, L. E.; Reich, K. A.; Sigman, D. S. *J. Am. Chem. Soc.* **1980**, *102*, 5419.

(40) (a) Johnson, G. R. A.; Nazhat, N. B. *J. Am. Chem. Soc.* **1987**, *109*, 1990. (b) Yamamoto, K.; Kawanisi, S. *J. Biol. Chem.* **1989**, *264*, 15435.

the minor groove for the phen and dpq species and at the major groove for the dppz species. The DNA bound copper(I) species is susceptible to react with  $\text{H}_2\text{O}_2$  to form  $[\text{Cu}^{\text{I}}(\text{Tp}^{\text{Ph}})(\text{L})]^+ \cdots \text{DNA}$  along with the formation of reactive hydroxyl radical, responsible for the DNA cleavage.<sup>41</sup>

## Conclusions

Four ternary copper(II) complexes having a tridentate tris-(3-phenylpyrazolyl)borate and bidentate heterocyclic base (L) are prepared and characterized. Crystal structures of the complexes show a spatial arrangement of three phenyl groups of  $\text{Tp}^{\text{Ph}}$  in forming a bowl-shaped structure that effectively encloses the  $\{\text{CuL}\}$  moiety. While the bpy and phen ligands essentially lie within the bowl, the extended quinoxaline and phenazine rings of dpq and dppz ligands stemmed outside the bowl. The space filling of the  $\text{Tp}^{\text{Ph}}$  ligand along with the ball-and-stick molecular model for the  $\{\text{CuL}\}$  moiety, obtained by BIOSYM INSIGHT (Version 97.5) in Silicon Graphics for complexes **1** and **4** containing bpy and dppz, respectively, show the extent of steric enclosure (Figure 6). The steric encumbrance has a profound effect on the DNA

binding and cleavage activity of complexes **1–4**. A significant observation is the higher propensity of dppz complex **4** in the cleavage of SC DNA compared to its phen and dpq analogues (**2**, **3**). Mechanistic investigations show a minor groove binding for the phen and dpq complexes, while the dppz complex binds at the major groove. Pathways involving hydroxyl radical in the DNA scission reactions are proposed from the observation of complete inhibition of the cleavage by DMSO.

**Acknowledgment.** This work is supported by the Department of Science and Technology, Government of India, and the Council of Scientific & Industrial Research, New Delhi. Thanks are due to the Alexander von Humboldt Foundation, Germany, for donation of an electroanalytical system and the Bioinformatic Center of Indian Institute of Science, Bangalore, for database search. P.A.N.R. thanks CSIR for a fellowship. We are thankful to Professor V. Raghavan for providing the Gel Documentation System facility.

**Supporting Information Available:** Listing of full crystallographic data, atomic coordinates, full list of bond distances and angles, anisotropic thermal parameters, and hydrogen atom coordinates for complexes **1–4** (CIF). This material is available free of charge via Internet at <http://pubs.acs.org>.

IC0201396

(41) Catalytic oxidation of ascorbic acid ( $\text{H}_2\text{A}$ ) by dioxygen involving a Cu(II)/Cu(I) redox couple is known to form  $\text{H}_2\text{O}_2$  in the buffer medium. Baron, E. S. G.; De Meio, R. H.; Klemperer, F. *J. Biol. Chem.* **1936**, *112*, 625.